

# Electrochemical Characterisation of Various Iron Species

J. Swaine

January 19, 2025

## Abstract

Understanding the electrochemical behaviours and characteristics of iron species is essential for their application in energy storage and electrocatalysis. In this study, 1 mM solutions of ferrocyanide, ferrocene methanol, and hydrated iron(II) sulphate were formed via dissolution in 0.1 M of  $\text{Na}_2\text{SO}_4$  electrolyte. Cyclic voltammograms were recorded using a carbon working electrode, a stainless steel counter electrode, and an Ag/AgCl reference electrode. Results were then analysed using Marcus theory. Graphs of peak oxidation current against the square root of scan rate were produced, and diffusion coefficients were determined for ferrocyanide in water and ferrocene in DCM, MeCN, and DMSO. These values were compared with literature data, sources of error were evaluated and an extensive rationalisation of the trend in viscosity and diffusion coefficient was performed. Further experiments examined 5 mM ferrocene carboxylic acid (FCA) in 0.1 M TBAPF<sub>6</sub>/MeCN, with and without a 5 mM ferrocene calibrant, to address the inaccuracy of a silver wire reference electrode. Results indicated that ferrocyanide and ferrocene methanol exhibit reversible electrochemical behaviour, with a peak oxidation current at 0.1 V s<sup>-1</sup> of  $i_p^{ox} = 16.40 \mu\text{A}$ , while ferrocene methanol showed the greatest reversibility ( $\Delta E = 0.06 \text{ V}$ ). Hydrated iron(II) sulphate was shown to be completely electrochemically irreversible. Diffusion coefficients deviated from literature values but were rationalised based on laboratory conditions. Equilibrium potential of FCA was determined as  $E_{eq} = 0.23 \text{ V}$  vs.  $\text{Fc}/\text{Fc}^+$ . Further investigation should aim to replicate the experimental conditions reported in the cited literature to achieve values in closer agreement, thereby enabling more confident application of experimental procedure to other solvent and electrolyte systems.

## 1 Method

One 0.1 M, 100 ml electrolyte solution was formed from  $\text{Na}_2\text{SO}_4$  (3.222 g, 0.01 mol) in deionised water. Three separate 25 ml, 1 mM solutions of ferrocyanide (0.011 g,  $2.5 \times 10^{-5}$  mol), ferrocene methanol (0.005 g,  $2.5 \times 10^{-5}$  mol), and hydrated iron(II) sulphate (0.007 g,  $2.5 \times 10^{-5}$  mol) were then formed via dissolution in the electrolyte. For each separate solution, a sample was taken and placed in an electrochemical cell. To the cell was attached, a working carbon electrode, a counter steel electrode, and a reference Ag/AgCl electrode. Before and after each measurement electrodes were polished thoroughly. Electrodes were connected to a potentiostat which was operated via PStrace software. The

following settings were used:  $E_{begin} = 0$  V,  $E_{vertex1} = 0.6$  V,  $E_{vertex2} = 0$  V,  $t_{equilibration} = 10$  s,  $E_{step} = 0.01$  V and no. of scans = 1. Scans were recorded at scan rates of  $0.01$  V s<sup>-1</sup>,  $0.02$  V s<sup>-1</sup>,  $0.05$  V s<sup>-1</sup>,  $0.1$  V s<sup>-1</sup>,  $0.2$  V s<sup>-1</sup> and  $0.5$  V s<sup>-1</sup>. Data was exported to Microsoft Excel for further processing. Next, an additional four, 25 ml solutions were formed. A 1mM solution of ferrocyanide in aqueous Na<sub>2</sub>SO<sub>4</sub> was prepared as before. For the three following solutions the electrolyte was formed by dissolving the TBAPF<sub>6</sub> salt with the following organic solvents: 50 ml of 0.1 M TBAPF<sub>6</sub>(1.937 g, 0.005 mol) in DCM, 100 ml TBAPF<sub>6</sub>(3.874 g, 0.01 mol) in MeCN, 50 ml TBAPF<sub>6</sub>(1.937 g, 0.005 mol) in DMSO. Each of these three solutions was then used as an electrolyte to form a 25 ml, 5mM ferrocene(0.023 g,  $1.25 \times 10^{-4}$ ) solution. One final 25 ml, 5mM ferrocene carboxylic acid(0.029 g,  $1.25 \times 10^{-4}$ ) solution was made using the TBAPF<sub>6</sub>/MeCN electrolyte. Measurements for each solution were performed in the electrochemical cell as before under the same settings, but this time the reference electrode was swapped to the Ag wire quasi-reference electrode. An additional measurement was performed for the ferrocene carboxylic acid system. Initially a measurement was performed as normal, having obtained a cyclic voltammogram, a quarter of the solution was then removed from the cell and replaced with a ferrocene TBAPF<sub>6</sub>/MeCN solution, where another measurement was then performed.

## 2 Results and discussion

### 2.1 Cyclic Voltammograms for Ferrocyanide, Ferrocene Methanol, and Hydrated Iron(II) Sulphate in Na<sub>2</sub>SO<sub>4</sub> Electrolyte and an Analysis Under Marcus Theory

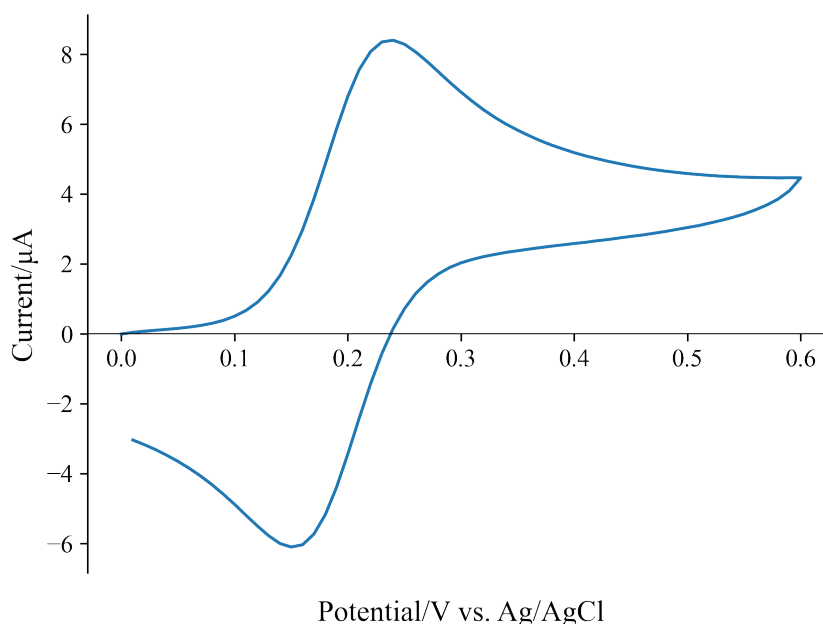


Figure 1: Cyclic Voltammogram of 1 mM ferrocyanide in 0.1 M Na<sub>2</sub>SO<sub>4</sub>, with a scan rate of  $0.1$  V s<sup>-1</sup> at 298 K.

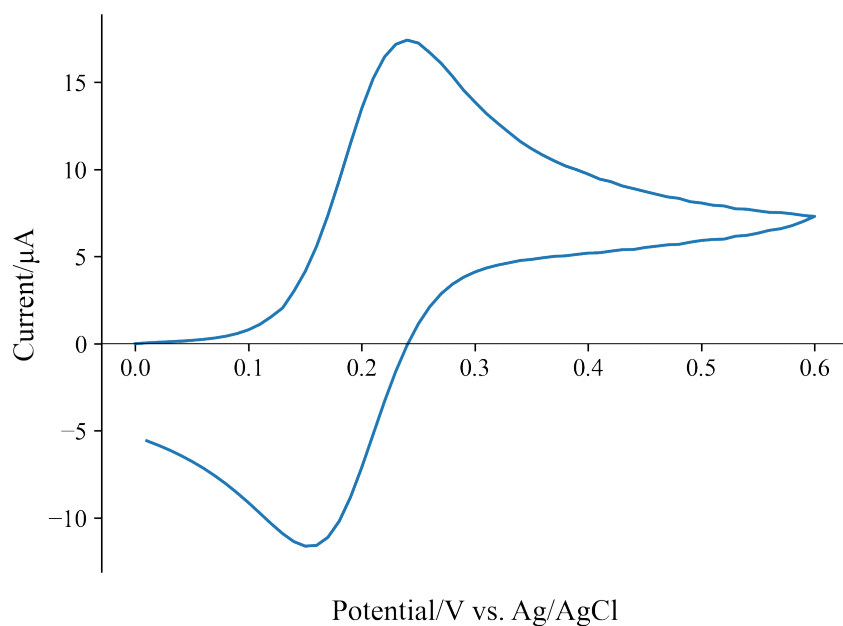


Figure 2: Cyclic Voltammogram of 1 mM ferrocene methanol in 0.1 M  $\text{Na}_2\text{SO}_4$ , with a scan rate of  $0.1 \text{ V s}^{-1}$  at 298 K.

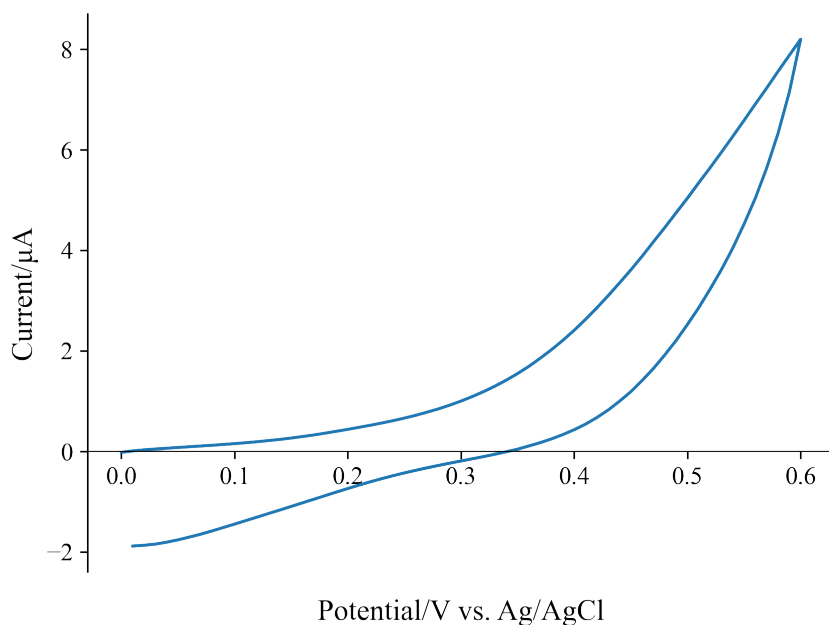


Figure 3: Cyclic Voltammogram of 1 mM hydrated iron (II) sulphate in 0.1 M  $\text{Na}_2\text{SO}_4$ , with a scan rate of  $0.1 \text{ V s}^{-1}$  at 298 K.

Ferrocenemethanol and ferrocyanide can be seen to display reversible behaviour, whilst aqueous iron (II) sulphate displays almost completely irreversible behaviour at a scan rate of  $0.1 \text{ V s}^{-1}$ .

The character of a redox reaction is well defined by the shape of the peaks in the cyclic voltammograms. In the case of ferrocyanide we note a strong forward peak at  $E_{ox} = 0.24$  V and an oxidation peak magnitude of  $i_p^{ox} = 7.65$   $\mu$ A, and a reduction peak at  $E_{red} = 0.18$  V with magnitude  $i_p^{red} = 6.96$   $\mu$ A. These well defined forward and backward peaks yield  $\Delta E = 0.06$  V. A value close to the expected value of  $\Delta E = 0.059$  V which characterises electrochemically reversible reactions.

Considering ferrocenemethanol, we observe a graph with a character that closely resembles ferrocyanide. The forward peak is seen at  $E_{ox} = 0.24$  V with an associated peak current of  $i_p^{ox} = 16.40$   $\mu$ A, and the backward peak is noted at  $E_{red} = 0.15$  V with a reduction peak magnitude of  $i_p^{red} = 12.49$   $\mu$ A. In this case the peak separation is greater than expected,  $\Delta E = 0.09$  V. This larger separation may be explained by the manifestation of electrode surface issues, such as an improperly polished electrode, the possible coupling of an additional reaction to the electron transfer introduced as a result of contaminants, slower ion movement impacting transfer kinetics, or it might suggest that the redox couple is beginning to display some quasi-irreversible behaviour.

For ferrocyanide and ferrocenemethanol, values were calculated by returning the voltage corresponding to the maximum/minimum value of  $\mu$ A for the forward and backward sweeps. The oxidation and reduction peaks were determined by extrapolating the baseline of the linear regions of the forward and reverse sweep and calculating the difference in the value of  $\mu$ A between the baseline and the peak at the same voltage. For electrochemically reversible reactions  $|i_p^{ox}| = |i_p^{red}|$ , but in this case the calculations yield deviation from this, increasing in size from ferrocyanide to ferrocenemethanol. Again, features of user error or not fully reversible behaviour.

Finally, for iron (II) sulphate we do not note the presence of a significant oxidation or reduction peak, indicating irreversible behaviour. The implication of this is that the redox reaction notes slow electron transfer kinetics preventing equilibration of the oxidised and reduced species at the electrode surface. This may be explained by many of the reasons considered previously to rationalise the larger  $\Delta E$  values of ferrocenemethanol.

The observed features can also be well understood on the basis of Marcus theory. Electron transfer will not occur until certain conditions have been met. Both species must have the same nuclear geometry and hence, be isoenergetic to one another, resulting in the donor HOMO and recipient LUMO being equal in energy. It is clear that there will be an energetic cost to achieving these conditions, this cost takes the form of the activation energy,  $\Delta G^\ddagger$ . Activation energy is dependent on free energy,  $\Delta G^\circ$ , and reorganisation energy  $\lambda$ . The physical implications of these features are that  $\Delta G^\ddagger$  is low for ferrocyanide and ferrocenemethanol and higher for iron (II) sulphate. Considering our first two species, we note what is likely to be a small  $\lambda$  implying low solvent reorganisation energy,  $\lambda_{outer}$ , and minor changes to bond geometry within the reactant and product,  $\lambda_{inner}$ , ultimately suggesting a greater similarity between the oxidised and reduced species in each case, respectively. A smaller  $\Delta G^\ddagger$  implies a larger value for  $k^\circ$ , and as given by the Butler-Volmer equation, will result in a larger current value,  $i$ . The opposite will hold true for iron (II) sulphate. It is unlikely that difference in system free energy will be large, as all experiments were conducted at ambient room temperature, so the difference can mainly be attributed to  $\lambda$ .

## 2.2 Peak Oxidation Current vs. Square Root of Scan Rate with a Rationalisation of Diffusion Coefficient Trends and Viscosity Effects

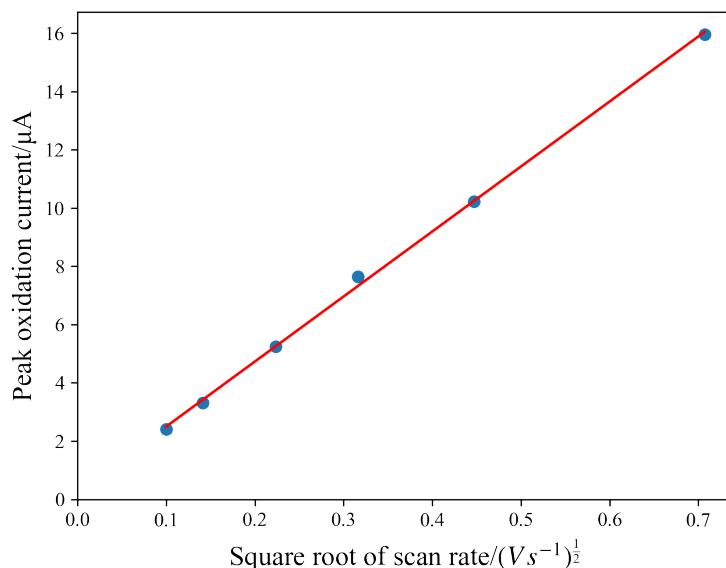


Figure 4: Graph showing the square root of the scan rate versus the peak oxidation current of 1 mM ferrocyanide in 0.1 M aqueous Na<sub>2</sub>SO<sub>4</sub> at 298 K. The red line represents the line of best fit.

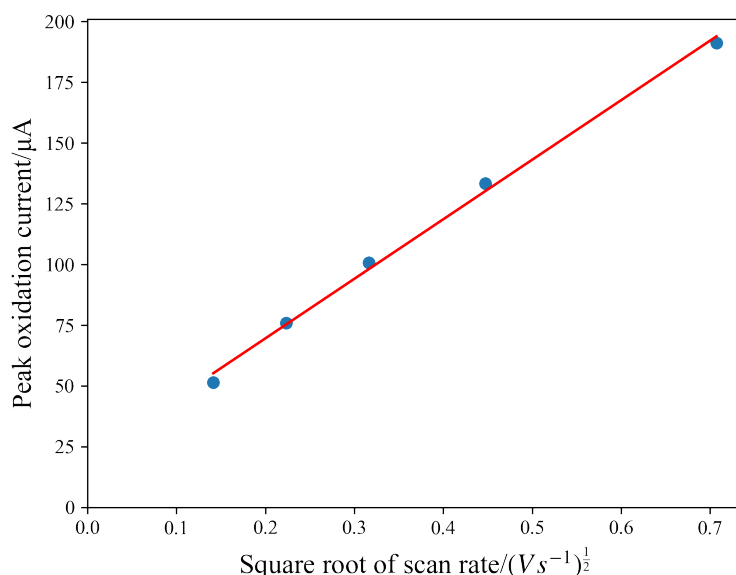


Figure 5: Graph showing the square root of the scan rate versus the peak oxidation current of 5 mM ferrocene in 0.1 M tetrabutylammonium hexafluorophosphate/dichloromethane at 298 K. The red line represents the line of best fit.

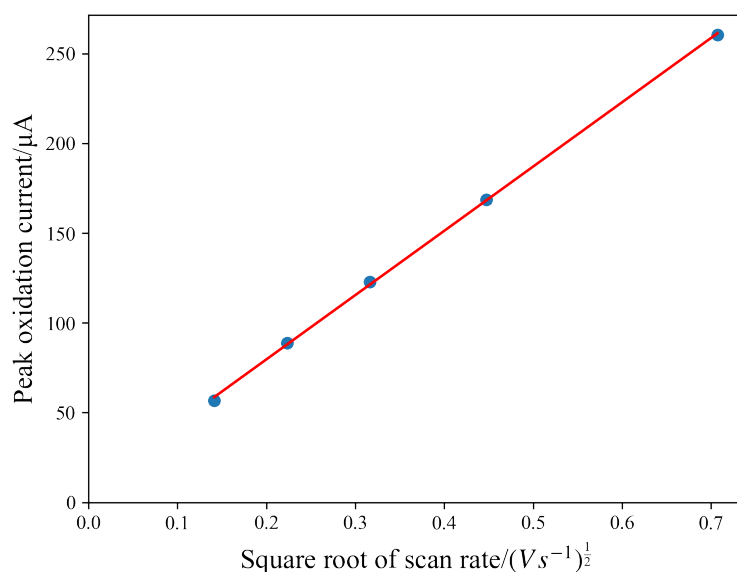


Figure 6: Graph showing the square root of the scan rate versus the peak oxidation current of 5 mM ferrocene in 0.1 M tetrabutylammonium hexafluorophosphate/acetonitrile at 298 K. The red line represents the line of best fit.

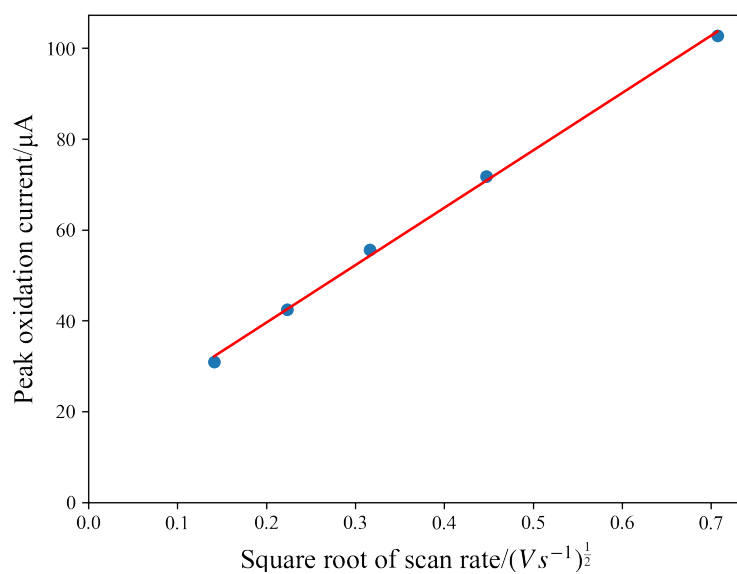


Figure 7: Graph showing the square root of the scan rate versus the peak oxidation current of 5 mM ferrocene in 0.1 M tetrabutylammonium hexafluorophosphate/dimethyl sulphoxide at 298 K. The red line represents the line of best fit.

The peak current  $i_p$  for a reversible electron transfer can be expressed as:

$$i_p = (2.69 \times 10^5) n^{3/2} A D^{1/2} c \nu^{1/2} \quad (1)$$

where:

- $n$  is the number of electrons transferred.
- $A$  is the electrode area ( $\text{m}^2$ ).
- $D$  is the diffusion coefficient ( $\text{m}^2 \text{s}^{-1}$ ).
- $c$  is the concentration ( $\text{mol m}^{-3}$ ).
- $\nu$  is the scan rate ( $\text{V s}^{-1}$ ).

Seeking the diffusion coefficient we can rearrange equation 1 as follows:

$$D = \left( \frac{i_p}{(2.69 \times 10^5) n^{3/2} A c \nu^{1/2}} \right)^2 \quad (2)$$

We note that equation 1 takes the linear form  $y = mx + b$ , where  $b = 0$ . We can therefore use the gradient of the line in question to solve for the diffusion rate.

$$D = \left( \frac{\text{gradient}}{(2.69 \times 10^5) n^{3/2} A} \right)^2 \quad (3)$$

Example calculation for Ferrocyanide in water:

$$D = \left( \frac{2.23 \times 10^{-5}}{(2.69 \times 10^5) \cdot (1)^{3/2} \cdot (7.07 \times 10^{-6})} \right)^2 \quad (4)$$

#### Diffusion coefficients:

1. Ferrocyanide in water:  $\mathbf{D_{calc}} = 1.38 \times 10^{-10} \text{m}^2 \text{s}^{-1}$
2. Ferrocene in DCM:  $\mathbf{D_{calc}} = 1.66 \times 10^{-8} \text{m}^2 \text{s}^{-1}$
3. Ferrocene in MeCN:  $\mathbf{D_{calc}} = 3.55 \times 10^{-8} \text{m}^2 \text{s}^{-1}$
4. Ferrocene in DMSO:  $\mathbf{D_{calc}} = 4.42 \times 10^{-9} \text{m}^2 \text{s}^{-1}$

Table 1: Table comparing calculated and literature diffusion coefficients at a temperature of 298K.

Redox Species	Solvent	$\mathbf{D_{calc}} \text{ (m}^2 \text{ s}^{-1}\text{)}$	$\mathbf{D_{lit}} \text{ (m}^2 \text{ s}^{-1}\text{)}$
Ferrocyanide	Water	$1.38 \times 10^{-10}$	$6.40 \times 10^{-10}$
Ferrocene	MeCN	$3.55 \times 10^{-8}$	$2.40 \times 10^{-9}$

The literature value for Ferrocyanide in water was taken from Moldenhauer et al. (2016)<sup>1</sup>, and the literature value for Ferrocene in MeCN was taken from Wang et al. (2010)<sup>2</sup>.

It can be seen that both the obtained experimental values deviate from the recorded literature values. The ferrocyanide and water system however, does offer agreement on the same order as the literature value, where as the value for Ferrocene in MeCN differs by a much greater margin.

It may be quickly understood where these errors arise from by considering the slightly different conditions under which the literature values were measured and the terms in the equation used to calculate the diffusion value. In Moldenhauer et al. (2016) the working electrode was platinum, the counter electrode was a platinum flag and the reference electrode was a saturated calomel electrode. Wang et al (2010) used a platinum working electrode, a silver wire reference electrode, and a platinum wire counter electrode. Differing experimental conditions provide reasonable explanation for diffusion coefficient discrepancy. In equation 3 we consider the variables "*gradient*", " $n^{3/2}$ ", and " $A$ ". Of these terms the only one that could have been significantly impacted as part of the laboratory conduct was the term, "*gradient*".

Defining gradient in this case:

$$m = (2.69 \times 10^5)n^{3/2}AD^{1/2}c \quad (5)$$

Given that the actual values associated with the derived linear equation, the values taken from the line of best fit for gradient,  $m$ , and intercept,  $b$ , were calculated using the python package NumPy and its polyfit function, we can say with some certainty, introduced error will not be the product of this operation. After visual inspection the only term that may offer insight into result deviation becomes the concentration term,  $c$ . During laboratory practice it is highly likely that the concentrations of electrolyte and redox species used are not precise due to a variety of features such as user error when weighing the masses of reagent to use, the reagents getting stuck to the glassware during transfer, or finally incomplete dissolution in general within the electrolyte or incomplete dissolution of the electrolyte itself (especially important in the case of low concentrations due to the overall proportion residual mass will make up) . This results in an incorrect concentration value being used for calculation of the peak oxidation value. Further sources of error and uncertainty may stem from the assumption that the aqueous electrolyte ion has no effect on the redox process. We also see by inspecting the obtained graphs that the lines of best fit clearly do not pass through the point 0,0 as the considered linear equation might suggest, another feature that should need accounting for in the calculation of the diffusion coefficient. Features such as electrode polishing and operation of the potentiostat with its associated software may also be a source of error however, appear minimal in comparison.

Table 2: Literature values for viscosity,  $\eta$ , compared to calculated diffusion coefficient values,  $D$ , at 298 K.

Solvent system	$\eta_{lit}$ (Pa · s)	$D_{calc}$ (m <sup>2</sup> s <sup>-1</sup> )
DCM	$4.13 \times 10^{-4}$	$1.66 \times 10^{-8}$
MeCN	$3.69 \times 10^{-4}$	$3.55 \times 10^{-8}$
DMSO	$1.97 \times 10^{-3}$	$4.42 \times 10^{-9}$

The viscosity values for DCM and MeCN were taken from Kennedy et al. (2004)<sup>3</sup> and the viscosity of DMSO was found in Alam et al. (2019)<sup>4</sup>.



Observing table 2, it is clear that larger values of  $\mathbf{D}_{\text{calc}}$  are associated with lower values of viscosity,  $\eta$ . In a qualitative light, we might first describe viscosity as the measure of a fluid's "thickness". Under this definition, we can relate the calculated diffusion and literature viscosity values to Marcus Theory. Following this, we might then construct a more rigorous answer for what is actually taking place.

The thickness of a solvent will affect its interactions with the redox species due to a more viscous medium impacting the rate of diffusion in the system, and hence, leading to a change in the activation energy,  $\Delta G^\ddagger$ , for the redox process. This interaction will manifest as part of the reorganization energy term,  $\lambda$ , more specifically the  $\lambda_{\text{outer}}$  term. Given that  $\Delta G^\ddagger$  can be related to  $\lambda_{\text{outer}}$  in the following way:

$$\Delta G^\ddagger = \frac{(\Delta G^\circ + \lambda_{\text{inner}} + \lambda_{\text{outer}})^2}{4(\lambda_{\text{inner}} + \lambda_{\text{outer}})} \quad (6)$$

where:

- $\Delta G^\ddagger$ : Activation energy for the electron transfer reaction, representing the minimum energy required to overcome the energetic barrier for the reaction.
- $\lambda_{\text{inner}}$ : Intramolecular reorganization energy.
- $\lambda_{\text{outer}}$ : Other contributions to energy such as solvent redistribution.
- $\Delta G^\circ$ : Standard Gibbs free energy change for the reaction.

If we increase the value of  $\lambda_{\text{outer}}$  we then increase the value of  $\Delta G^\ddagger$ . Then, making the assumption that our system displays arrhenius type behaviour, a rate constant for electron transfer,  $k_{\text{ET}}$ , can be expressed as a function of  $\Delta G^\ddagger$ .

$$k_{\text{ET}} = A_{\text{exp}} \exp\left(-\frac{\Delta G^\ddagger}{RT}\right) \quad (7)$$

where:

- $k_{\text{ET}}$  is the electron transfer rate constant.
- $A_{\text{exp}}$  is the pre-exponential factor.
- $R$  is the gas constant.
- $T$  is the temperature in Kelvin.

It is clear to see that a large value of  $\Delta G^\ddagger$  will decrease the value obtained for  $k_{\text{ET}}$ . As such we will note the following relationships:

$$i = AFj, \quad j = k_{\text{ET}}[\text{Reactant}] \quad (8)$$

where:

- $A$ : Area of the electrode ( $\text{m}^2$ )
- $F$ : Faraday's constant ( $\text{C mol}^{-1}$ )
- $j$ : Flux of the reactant at electrode ( $\text{mol cm}^{-2} \text{s}^{-1}$ )

- $[Reactant]$ : Concentration of the reactant.

We may then consider the following transformation:

$$i = AFk_{ET}[Reactant] \quad (9)$$

$$\implies i = AFA_{exp} \exp\left(-\frac{\Delta G^\ddagger}{RT}\right) [Reactant] \quad (10)$$

Equations 9 and 10 show explicitly the relationship between  $\Delta G^\ddagger$  and  $i$ . So if we were to see an increase in the value of  $\lambda_{outer}$ , we would also see increase in  $\Delta G^\ddagger$ , where we would then expect to see a decrease in  $i$ .

We can then link this to viscosity. Let us first define the Stokes-Einstein equation:

$$D = \frac{k_b T}{6\pi\eta a} \quad (11)$$

Where:

- $D$ : Diffusion coefficient ( $\text{m}^2/\text{s}$ ).
- $k_b$ : Boltzmann constant.
- $\eta$ : Viscosity ( $\text{Pa s}$ ).
- $a$ : Molecular radius ( $\text{m}$ ).

A clear observation is that increasing the value of  $\eta$  will decrease the value of  $D$ . We must then also consider Fick's first law of diffusion:

$$j = -D \frac{\partial[B]}{\partial x} \quad (12)$$

where:

- $[B]$ : Bulk concentration ( $\text{mol m}^{-3}$ )
- $x$ : Displacement ( $\text{m}$ )

Seeing flux,  $j$ , is clearly dependent on diffusion,  $D$ , we can now refer back to 8. We see that a decreased value of  $D$  will result in a lower value of  $j$ , and hence a lower value  $i$ .

At peak current, where the rate of electron transfer is at a maximum, the considered system becomes limited by the diffusion of the redox species to the electrode. We can now refer back to equations 1, 2, and 3 used to obtain  $\mathbf{D}_{calc}$ , and clearly note that, all other terms constant, at a lower value of  $i_p$ , we expect  $\mathbf{D}_{calc}$  to be low, and if we expect  $\mathbf{D}_{calc}$  to be low then we expect  $\eta$  to be higher. High  $\eta$  then corresponding to the physical property of a "thicker" medium. The features of these equations fully justify the observed trend in  $\mathbf{D}_{calc}$  versus  $\eta_{lit}$ .

## 2.3 The impact of a quasi-reference electrode on equilibrium potential

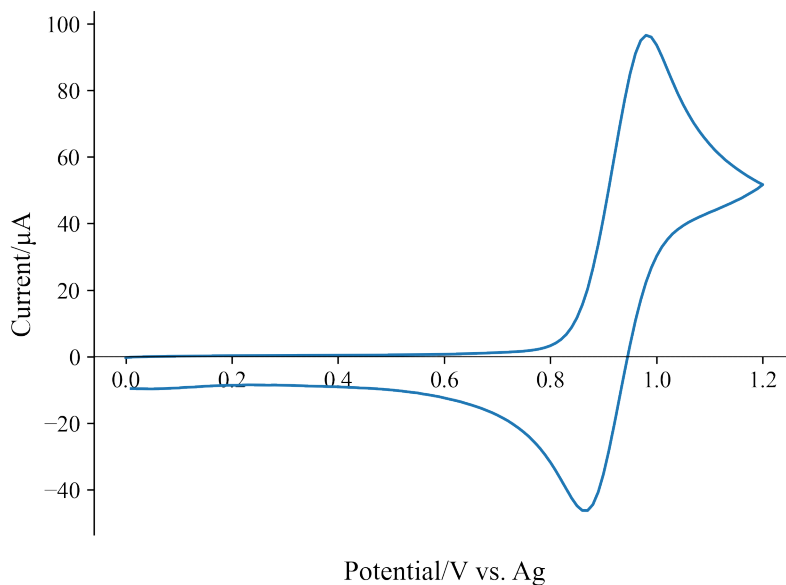


Figure 8: Cyclic Voltammogram of 5 mM ferrocenecarboxylic acid in 0.1 M tetrabutylammonium hexafluorophosphate/acetonitrile with a scan rate of  $0.1 \text{ V s}^{-1}$  at 298 K.

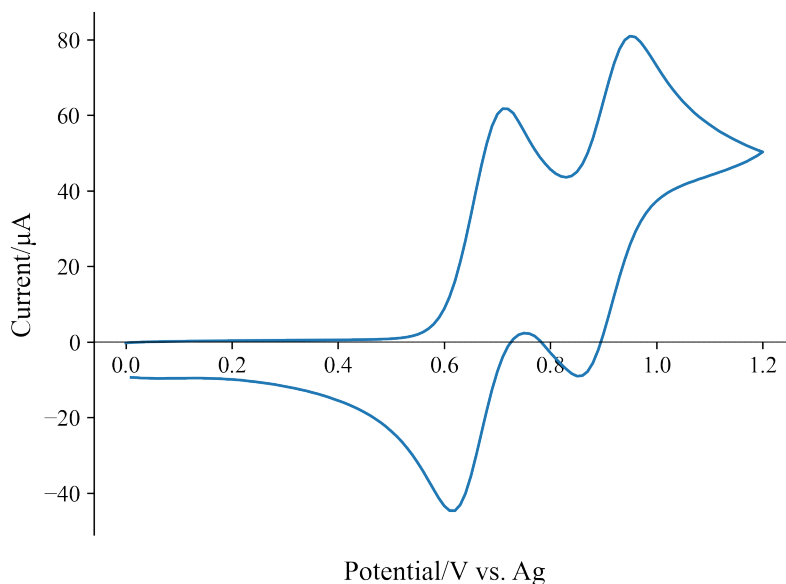


Figure 9: Cyclic Voltammogram of 5 mM ferrocenecarboxylic acid and 5 mM ferrocene in 0.1 M tetrabutylammonium hexafluorophosphate/acetonitrile with a scan rate of  $0.1 \text{ V s}^{-1}$  at 298 K.

Potentials are given by the following equation:

$$E_{\text{eq}} = \frac{E_{\text{ox}}^p + E_{\text{red}}^p}{2} \quad (13)$$

Where:

- $E_{\text{ox}}^p$  is the oxidation peak potential,
- $E_{\text{red}}^p$  is the reduction peak potential.

$E_{\text{eq}}$  vs.  $\text{Fc}/\text{Fc}^+$  is given by the following equation:

$$E_{\text{eq}} = E(\text{FCA}) - E(\text{Fc}/\text{Fc}^+) \quad (14)$$

Equilibrium potentials:

$$E_{\text{eq}} \text{ vs. Ag for FCA} = 0.90 \text{ V} \quad (15)$$

$$E_{\text{eq}} \text{ vs. Fc}/\text{Fc}^+ \text{ for FCA} = 0.23 \text{ V} \quad (16)$$

$E$  vs.  $\text{Fc}/\text{Fc}^+$  is a more reliable value to quote due to the nature of the silver reference electrode used. A silver wire is a quasi-reference electrode, meaning it will see variation in its potential dependent on the experimental conditions. This variation will make results difficult to compare to literature values. The use of a calibrant allows a new potential calculation to be performed relative to that of the calibrant, allowing more reproducible and consistent results that are not subject to fluctuation in silver's potential. Additionally, silver wire may become tarnished if it itself takes part in reaction becoming oxidised, further contributing to deviations in its potential across different experiments.

It is not possible to use the  $\text{Ag}/\text{AgCl}$  electrode in its place as despite a more stable potential, the aqueous environment required to stabilise this potential cannot be used with other solvents.

If both values are considered to be "vs. Ag", it can be seen that  $E_{\text{eq}}$  for FCA is greater than that of Ferrocene a value of 0.90 V compared to 0.67 V. This can be rationalised by understanding the chemical structures of the species involved. The important difference between the two species is the addition of a carboxylic acid group ( $-\text{COOH}$ ) on FCA. The carboxylic acid group is an electron withdrawing group and so acts to decrease the electron density on the Cp ring and hence the central iron atom. The effect of this is that the withdrawal of electron density makes the Fe (III) oxidation state more stable relative to that of the Fe (II) oxidation state, influencing the system to favour oxidation. In favouring oxidation, a more positive redox potential is then noted, and hence the peak appears at more positive potential on the CV. This culminates in a larger value of  $E_{\text{eq}}$  for FCA than Fc, when considering both with respect to the Ag reference electrode. The Cp ligand itself is electron donating, meaning that when compared against its carboxylated derivative it will stabilise a more electron rich metal centre – the Fe (II) centre. The effect of this is the converse of that stated above. The system comparatively favours reduction hence observes a more negative potential resulting in the smaller (more negative) value of  $E_{\text{eq}}$ .

### 3 Conclusion

The study demonstrated that ferrocyanide and ferrocene methanol exhibit reversible electrochemical behaviour, while hydrated iron(II) sulphate displays irreversible character.

The electrochemical properties of these species were effectively analysed using Marcus Theory. Plots of peak oxidation current versus the square root of scan rate revealed reasonable linearity, supporting the applicability of the Randles-Ševčík equation. Diffusion coefficients were calculated for four systems, with values for ferrocyanide in water ( $1.38 \times 10^{-10} \text{ m}^2 \text{ s}^{-1}$ ) and ferrocene in MeCN ( $3.55 \times 10^{-8} \text{ m}^2 \text{ s}^{-1}$ ) compared to literature data. Deviations of  $5.02 \times 10^{-10} \text{ m}^2 \text{ s}^{-1}$  and  $3.31 \times 10^{-8} \text{ m}^2 \text{ s}^{-1}$ , respectively, were noted, and potential sources of error, such as experimental conditions and electrode calibration, were identified and discussed. The relationship between viscosity and diffusion coefficient was explored, providing insights into the role of the solvent in electrochemical behaviours. Additionally, a quasi-reference electrode was investigated using two electrochemical systems, pure ferrocene carboxylic acid in TBAPF<sub>6</sub>/MeCN and ferrocene carboxylic acid plus ferrocene in TBAPF<sub>6</sub>/MeCN, enabling the calculation of equilibrium potential values for both calibrated and non-calibrated setups with values of  $E_{\text{eq}} = 0.23 \text{ V vs. Fc/Fc}^+$  and  $E_{\text{eq}} = 0.9 \text{ V vs. Ag}$ . These findings highlight the importance of precisely replicating experimental conditions to ensure accurate and reproducible results, while providing valuable insights into the differing characteristics of electrochemically reversible and irreversible systems.

## References

- [1] J. Moldenhauer, *Journal of The Electrochemical Society*, 2016, **163**, 672.
- [2] Y. Wang, E. I. Rogers and R. G. Compton, *Journal of Electroanalytical Chemistry*, 2010, **648**, 15–19.
- [3] K. Kennedy and D. Miles, *Journal of Undergraduate Chemistry Research*, 2004, **4**,.
- [4] S. Alam, B. Ashokkumar and M. Siddiq, *Journal of Molecular Liquids*, 2019, **281**, 584–597.
- [5] C. Saouma, W. Morris and J. Darcy, *National Library of Medicine*, 2015, **25**, 9256–9260.